International Journal of Pharmaceutics 421 (2011) 388–396

Contents lists available at SciVerse ScienceDirect

International Journal of Pharmaceutics

journal homepage: www.elsevier.com/locate/ijpharm

Pharmaceutical Nanotechnology

Facile synthesis of pH sensitive polymer-coated mesoporous silica nanoparticles and their application in drug delivery

Hongyan Tang[a], Jia Guo[a], Yang Sun[b], Baisong Chang[a], Qingguang Ren[b], Wuli Yang[a,*]

[a] Key Laboratory of Molecular Engineering of Polymers (Ministry of Education) and Department of Macromolecular Science, Fudan University, Shanghai, 200433, China
[b] Center of Analysis and Measurement, Fudan University, Shanghai 200433, China

ARTICLE INFO

Article history:
Received 20 July 2011
Received in revised form 3 September 2011
Accepted 2 October 2011
Available online 6 October 2011

Keywords:
Mesoporous silica nanoparticle
pH sensitive
Composite microsphere
Drug delivery

ABSTRACT

pH-responsive polymer shell chitosan/poly (methacrylic acid) (CS-PMAA) was coated on mesoporous silica nanoparticles (MSN) through the facile *in situ* polymerization method. The resultant composite microspheres showed a flexible control over shell thickness, surface charges and hydrodynamic size by adjusting the feeding amount of MSN and the molar ratio of [$-NH_2$]/MAA. The MSN/CS-PMAA composite microspheres were stable in the pH range of 5–8 as well as in the physiological saline (0.15 M NaCl). Doxorubicin hydrochloride (DOX) was applied as a model drug to investigate the drug storage and release behavior. The results demonstrated that DOX could be effectively loaded into the composite microspheres. The cumulative release of DOX-loaded composite microspheres was pH dependent and the release rate was much faster at low pH (5.5) than that of pH 7.4. The cytotoxicity test by MTT assay showed that the blank carrier MSN/CS-PMAA microspheres were suitable as drug carriers. The cellular uptake of composite microspheres was investigated by confocal laser scanning microscopy (CLSM), which indicated that MSN/CS-PMAA could deliver the drugs into HeLa cell. The above results imply that the composite microspheres are a promising drug delivery system for cancer therapy.

1. Introduction

In the past decades, to protect the healthy tissues/organs such as kidney, liver, bone marrow and heart from the toxic drugs and prevent the denaturing of the drugs prior to reaching the targeted intracellular and intranuclear regions, the stimuli-responsive drug delivery carriers have been widely designed (Stuart et al., 2010). These "smart" drug delivery systems are susceptible of a rapid response to the changes of local environment, such as temperature, pH, light and magnetic field (Schmaljohann, 2006; Liu et al., 2006; Qiu and Park, 2001; Medeiros et al., 2011). Among the controlled drug delivery systems, pH sensitive system is of special interest in view of the fact that both extracellular tumor (pH 6.8) (Engin et al., 1995) and endosomes (pH 5.5) (Lee and Oh, 2007) are more acidic than normal tissues (pH 7.4). Mesoporous silica nanoparticles (MSN) have been extensively explored as drug delivery systems due to their superior properties such as high pore volume, large surface area, prominent biocompatibility, accessible surface functionalization and providing protection for the payloads (Vallet-Regi et al., 2007; Lu et al., 2010; Vallet-Regi et al., 2001; Singh et al., 2011; Ashley et al., 2011). However, if without appropriate surface modification, MSN are unable to intelligently deliver drugs in a targeted and controlled manner. With an aim to administer drug molecules specifically toward target tissues, pH sensitive molecules have been introduced to prepare hybrid nanoparticles with MSN.

To date, several research groups have taken great efforts to explore supramolecular and molecular machines coated porous structure to allow for the pH-dependent release of drugs. Zink et al. did a variety of research to employ supramolecular system as pH responsive nanovalves attached on the surface of mesoporous silica (Angelos et al., 2008; Zhao et al., 2010; Meng et al., 2010). Martinez-Manez et al. (Aznar et al., 2009) developed the pH-controlled "open-close" mesoporous materials comprising the functional moieties of polyalcohol and boronic acid groups. Also, propyldiethylenetriamine (multiamine chains) was investigated in their group as an alternative to functionalize mesopores for tailoring the release of guest molecules (Casasus et al., 2004). Along this line, Xu et al. (Gao et al., 2010) studied the effect of multiamine chains on the controlled drug release. Apart from the decoration of MSN with small molecules, the use of polymer-coated MSN also played an important role in the development of such systems, because polymers can provide tailored properties of biocompatibility, stability, size, structure, and functionality and when applied as drug delivery system, polymer-based materials can facilitate higher payloads, prolong the circulation time of drugs, improve drug targeting and solubility, and provide controlled release of the

* Corresponding author at: Key Laboratory of Molecular Engineering of Polymers and Department of Macromolecular Science, Fudan University, No. 220 Handan Road, Shanghai 200433, China. Tel.: +86 21 6564 2385, fax: +86 21 6564 0293.
E-mail address: wlyang@fudan.edu.cn (W. Yang).

0378-5173/$ – see front matter © 2011 Elsevier B.V. All rights reserved.
doi:10.1016/j.ijpharm.2011.10.013

therapeutics into the blood stream or the targeted tumor tissues (Wang et al., 2008; Liu et al., 2009). Linear polymers such as poly (acrylic acid) (PAA) (Hong et al., 2009) and poly (methacrylic acid) (PMAA) (Gao et al., 2009) chains were grafted onto the surface of MSN to serve as pH sensitive gatekeeper, at high pH value, the gate was open and the guest molecules were released due to the extending of polymer chains while in acidic medium, the polymers compacted and blocked the release of loaded drug. However, the above-mentioned pH-sensitive drug release mechanism was not suitable for practice operation because the medium of cancerous tissue or endosome/lysosome was more acidic than that of normal tissues.

To the best of our knowledge, most reported polymer-MSN hybrid materials have been fabricated by three methods: (a) layer-by-layer adsorption technique, which was based on electrostatic attraction to assemble multilayered polyelectrolytes on the surface of MSN (Wang et al., 2005); (b) "graft from" strategy, such as free radical polymerization and ATRP (Carniato et al., 2010); (c) "graft to" strategy, of which surface-initiated polymerizations initiated by functional groups on cores, such as –OH, $–NH_2$, $–CH{=}CH_2$, and –R –Br, etc. (Liu et al., 2011). Despite the success of these approaches, there are still some drawbacks, such as tedious multiple-step syntheses, necessity of suitable surfactants, very low surface grafting efficiency or encapsulation efficiency, etc. (Fleming et al., 2001). Therefore, it is still a challenge work to explore a simple and facile method to prepare drug carriers that would be capable of recognizing the intrinsic pH differences between cancers and normal tissues and can present faster release behavior at low pH.

Saccharides have been widely used as conjugate materials due to the outstanding characteristics of biocompatible, biodegradable and hydrophilic as well as the possibility of coating particles with specific ligands (Revilla et al., 1995; Baldwin and Kiick, 2009; Pichot, 2004). Chitosan is such a versatile bio-polysaccharide (He et al., 1999; Pan et al., 2002) that has been caused much attention (Guo et al., 2008; Wu et al., 2006). Herein, we proposed a facile and efficient strategy to synthesize pH responsive nanocarriers with chitosan-poly (methacrylic acid) (CS-PMAA) shells and MSN cores via *in situ* polymerization approach. This route was based on a one-pot strategy without requiring separation steps. The physicochemical and pH sensitive properties of MSN/CS-PMAA composite microspheres were analyzed. Doxorubicin hydrochloride (DOX), a classic anticancer drug, was chosen as a model drug to assess the drug loading and releasing behaviors. The cellular uptake and cytotoxicity test of MSN/CS-PMAA to HeLa cells were also performed.

2. Material and methods

2.1. Materials

Chitosan with the deacetylation degree of 90% and the molecular weight of 200 kD was purchased from Kabo Biochemical Company (Shanghai, China). Methacrylic acid (MAA) (Shanghai Chemical Reagents Company, Shanghai, China) was distilled under reduced pressure in nitrogen atmosphere. Potassium persulfate ($K_2S_2O_8$) was recrystallized from distilled water. Tetraethyoxysilane (TEOS), cetyltrimethylammonium bromide (CTAB), sodium hydroxide (NaOH) were obtained from Shanghai Chemical Reagents Company. Doxorubicin (DOX) in the form of hydrochloride salt was obtained from Beijing Huafeng United Technology Company. MTT (3-(4,5-dimethylthiazol-2-yl)-2,5-diphenyltetrazolium bromide) assay and other biological reagents were purchased from Invitrogen Corp. All other reagents were of analytical grade and used without further purification.

2.2. Preparation of mesoporous silica nanoparticles

Mesoporous silica nanoparticles (MSN) were prepared according to the sol–gel method (Slowing et al., 2007). Briefly, 0.5 g CTAB and 0.14 g NaOH were mixed in 240 mL deionized water. The solution was stirred vigorously at 80 °C for 2 h and 2.5 mL TEOS was added to react for another 2 h. Then the as-prepared product (MSN-CTAB) was washed with ethanol for 3 times and redispersed in ethanol solution of NH_4NO_3 (200 mL, 10 mg/mL) at 80 °C to remove the template of CTAB. The mixture was refluxed for 6 h, collected by centrifugation and washed with ethanol repeatedly. Finally, the obtained MSN was dried under vacuum to give the white powder.

2.3. Preparation of MSN/CS-PMAA composite microspheres

First, 0.16 g MSN was added to 30 mL of aqueous solution containing 0.2 g CS and 0.43 g MAA with a molar ratio of 1:4 ([glucosamine unit]:[MAA], i.e. $[–NH_2]$/[MAA]). The concentration of MSN in the system was fixed at 5 g/L (except when otherwise stated). The reaction mixture was ultrasonicated for 20 min, then stirred under nitrogen environment for 0.5 h, and heated to 80 °C. After the temperature remained at 80 °C for 10 min, the solution became clear, $K_2S_2O_8$ was added to the reaction mixture, and the concentration of $K_2S_2O_8$ in the mixture system was about 4.0×10^{-3} mol/L. The reaction was maintained at 80 °C under a nitrogen atmosphere for another 2 h with the rotative velocity speed of mechanical stirrer at 300 rpm. During this period, the milk white color in the reaction mixture disappeared and became light yellow. Afterward, the system temperature was lower from 80 °C to 50 °C. Then, 0.1 mL glutaraldehyde (0.25 wt%) was added to the system, after about 10 min, the color of the reaction mixture changed from light yellow to brown. The reaction was continued for another 2 h to proceed it completely. The obtained products were washed by deionized water for 3 times.

2.4. DOX loading and release

DOX was dissolved in distilled water with a concentration of 1 mg/mL. 5 mg of MSN/CS-PMAA composite microspheres was ultrasonically dispersed in 1.5 mL of the DOX solution. Therefore, the weight ratio of the drug to the composite microspheres was 0.3. The mixture was stirred at room temperature for 24 h. Then the dispersion was centrifuged at 14,000 rpm for 10 min to collect the DOX-loaded composite microspheres. The supernatant was kept for calculating the drug loading content. The amount of DOX loaded in the composite microspheres was analyzed by UV at the wavelength of 480 nm. The drug loading content and entrapment efficiency were calculated using the formulas (1) and (2), respectively:

$$\text{Loading content } (\%) = \frac{\text{initial amount of DOX} - \text{supernatant free amount of DOX}}{\text{DOX loaded composite microspheres}} \times 100\% \quad (1)$$

$$\text{Entrapment efficient } (\%) = \frac{\text{initial amount of DOX} - \text{supernatant free amount of DOX}}{\text{Initial amount of drug}} \times 100\% \quad (2)$$

To study the release behavior, DOX-loaded composite microspheres were re-dispersed in 4 mL distilled water. 0.5 mL of the dispersion was then transferred into a dialysis bag (cut off molecular weight 14,000 g/mol) followed by the addition of another 0.5 mL distilled water to avoid residues in apparatus. The bag was subsequently placed in a 200 mL PBS solution at 37 °C. At appropriate time intervals, 2 mL solution was collected and at the same time,

2 mL of the fresh PBS solution was added to keep the volume of the release medium constant. Three pH values of 5.5, 6.8 and 7.4 were used to simulate the different biological environments. The amount of DOX in the release medium was measured by UV at the wavelength of 480 nm. All measurements were performed in triplicate. The releasing content was calculated by the formula (3):

$$\text{Releasing content } (\%) = \frac{\text{amount of drug in the release medium}}{\text{amount of drug loaded into composite microspheres}} \times 100\% \quad (3)$$

2.5. Cytotoxicity assays

A human cervical cancer cell line (HeLa cells) was used to evaluate the cytotoxicity of MSN/CS-PMAA and DOX@MSN/CS-PMAA. HeLa cells were cultured in a RPMI-1640 medium supplemented with 10% (v/v) fetal bovine serum, 2 mM L-glutamine, 100 U/mL penicillin and 100 U/mL streptomycin at 37 °C and 5% CO_2. The cytotoxicity was assessed using MTT (3-(4,5-dimethylthiazol-2-yl)-2,5-diphenyltetra-zolium bromide) assay. Cells were seeded into 96-well microtiter plates at the density of 20,000 cells per well. After incubation for 24 h, the medium was aspirated and various concentrations of samples (free DOX, DOX-MSN@CS-MAA and MSN@CS-MAA) in fresh cell growth medium were added. Control cells were added with equivalent volume of fresh media. Cells were cultured for 24 h before the cell viability assay was performed. The old medium was removed and 100 μL of fresh medium and 10 μL of a 5 mg/mL MTT solution were added to each well. Plates were then incubated under cell culture conditions for 4 h. The old medium was aspirated and 100 μL DMSO was added to dissolve the formazan crystals. The absorbance of each sample was measured at 570 nm with a background correction at 630 nm.

2.6. In vitro cellular uptake

HeLa cells were plated in cell culture dish using RPMI-1640 medium supplemented with 10% (v/v) fetal bovine serum, 2 mM L-glutamine, 100 U/mL penicillin and 100 U/mL streptomycin at 37 °C and 5% CO_2. The medium was then replaced with 1 mL culture serum-free medium containing FITC-labeled samples. After incubation for 3 h, the culture medium was removed and the cells in cell culture dish were washed three times with PBS. Fluorescence images of cells were obtained using confocal microscope (Leica TCS SP5).

2.7. Characterization

Transmission electron microscopy (TEM) images were obtained on a Hitachi H-600 transmission electron microscope, and the samples for TEM measurements were prepared by placing one drop of sample on copper grids covered with carbon. Samples were dried at room temperature, and then were examined on TEM without being stained. The mean size and size distribution (PI = $\langle\mu_2\rangle/\Gamma^2$ (Chu et al., 1991)) of the particles were measured by dynamic light scattering (DLS) (Malvern, Autosizer 4700) in aqueous solution with pH 7.4 (except when otherwise stated). All DLS measurements were carried out with a wavelength of 532 nm at 25 °C and an angle detection of 90°. The zeta potential of the particles was measured on a Zetasizer Nano-ZS (Malvern) at 25 °C. All measurements were performed in triplicate. Powder X-ray diffraction (PXRD) patterns were recorded on a Bruker D4 X-ray diffractometer with Ni-filtered Cu KR radiation (40 kV, 40 mA). Nitrogen adsorption–desorption isotherms were obtained on a Micromeritics ASAP 2000 pore analyzer at 77 K under continuous adsorption conditions. Brunauer–Emmett–Teller (BET) and Barrett–Joyner–Halenda (BJH) analyses were used to calculate the surface area, pore size, and pore volume, respectively. FTIR spectra were measured on a Nicolet Nexus-440 FTIR spectroscopy. All measured samples were dried, and the powders were mixed with KBr and pressed to a plate for measurement. Thermogravimetric analysis of microspheres was measured on Pyris 1 TGA instrument with a heating rate of 20 °C/min and air environment.

Table 1
Particle size and zeta potential of MSN and MSN/CS-PMAA composite microspheres.[a]

Sample	Zeta potential (mV)	Hydrodynamic diameter (nm)[b]	PI[c]
MSN	−28.8	241	0.02
MSN/CS-PMAA	−50.2	358	0.09

[a] All the data was measured at pH 7.4 and 0.15 M sodium phosphate buffer solution.
[b] The diameter was determined at 25 °C by DLS.
[c] PI, polydispersity index, PI = $\langle\mu_2\rangle/\Gamma^2$.

3. Results and discussion

3.1. Preparation of MSN/CS-PMAA composite microspheres

In this paper, we developed an *in situ* approach to encapsulate CS-PMAA on the surface of MSN, creating pH sensitive microspheres by a one-pot route. In acidic condition, CS molecules were cationic polyelectrolytes and assembled with MAA to form polymer–monomer pair, which could be coated on the surface of MSN nanoparticles via electrostatic interaction to form CS/nanoparticle complexes, and then CS/nanoparticle complexes were utilized as templates for the subsequent polymerization of methacrylic acid, during this process, CS was interpenetrated with PMAA chains to form the physically crosslinked networks on the MSN. As such, the core–shell composite microspheres were formed eventually and could be well dispersed in aqueous solution due to the strong associations among the CS-PMAA chains through hydrogen bonding and physical entanglements (De Vasconcelos et al., 2006; Colombo et al., 2009).

Fig. 1 showed the representative TEM images of MSN and MSN/CS-PMAA microspheres. Fig. 1(a) displayed the typical MSN particles with the mean diameter of 110 ± 10 nm. In contrast, Fig. 1(b) visualized the thin gray outer around the MSN, implying the presence of organic moieties that completely covered the MSN core. Table 1 listed the hydrodynamic diameters, size distributions (polydispersity index, PI = $\langle\mu_2\rangle/\Gamma^2$ (Chu et al., 1991) was measured by dynamic light scattering (DLS) Malvern, Autosizer 4700) and zeta potentials of MSN and MSN/CS-PMAA composite microspheres, respectively. MSN with the hydrodynamic diameter of 241 nm was smaller than that of MSN/CS-PMAA (358 nm). Additionally, the hydrodynamic size of MSN/CS-PMAA was obviously larger than that shown in TEM image because of the hydrate layer in aqueous environment. The zeta potential of MSN was −28.8 mV. Due to the successful encapsulation of CS-PMAA, the zeta potential of MSN/CS-PMAA was decreased to −50.2 mV, which indicated the existence of a great amount of carboxyl groups. All these results proved that the CS-PMAA polymer shells were formed and provided higher charge density to make the composite microspheres sufficiently stable in aqueous environment.

Powder X-ray diffraction (PXRD) was conducted to determine the structures of MSN. The PXRD pattern in Fig. 2(a) showed three main diffraction peaks due to (1 0 0), (1 1 0), and (2 0 0) planes, respectively, which well corresponded to the typical diffraction peaks of hexagonal mesoporous structure (Beck et al., 1992). The total surface area and average pore diameter of MSN and MSN/CS-PMAA were analyzed by the N_2 adsorption and desorption measurements. The BET isotherms of these two materials in Fig. 2(b) displayed typical IV isotherm according to the IUPAC

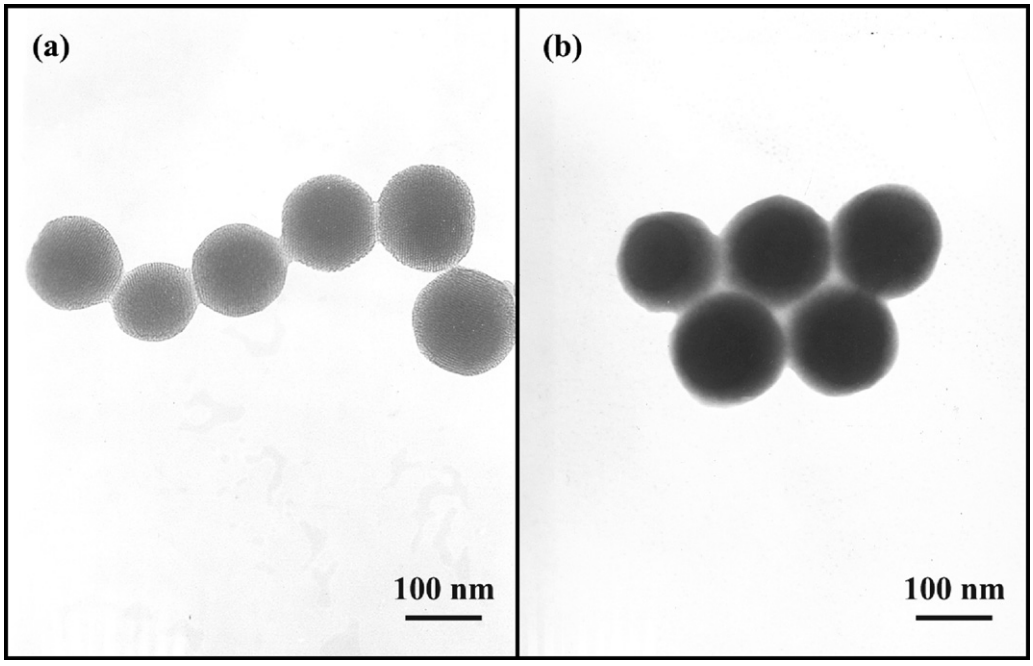

Fig. 1. TEM micrographs of MSN (a) and MSN/CS-PMAA composite microspheres (b).

classification, showing the characteristic of mesopores. Compared with MSN, the adsorbed nitrogen amount of MSN/CS-PMAA was reduced, but the shape of the hysteresis loop remained unchanged. The surface area, pore volume and pore diameter of MSN were 946 m^2/g, 1.32 cm^3/g and 3.2 nm, respectively. After being coating with polymer, these parameters were reduced to 682 m^2/g, 0.87 cm^3/g and 2.6 nm, respectively. This result suggested that the pore shape was not significantly destructed after polymer coating and polymer was distributed predominantly on the exterior surface of MSN, which specified that the retained mesoporosity could provide space to accommodate drug molecules.

Fig. 3 showed FTIR spectra of CS, MSN and MSN/CS-PMAA. As expected, chitosan revealed typical peaks of 1596 cm^{-1} (amide II) and 1384 cm^{-1} (amide III) (Schiffman and Schauer, 2007). In the spectrum of MSN, C–H stretch (2854 cm^{-1} and 2923 cm^{-1}) peaks from CTAB surfactants disappeared after the CTAB removal process, which indicated that no residual CTAB existed in the material, so the impact of the toxicity from CTAB was eliminated. In the spectrum of MSN/CS-PMAA, when compared with those of CS and MSN, the characteristic absorption bands were found to appear at 1720 cm^{-1}, 1628 cm^{-1} and 1100 cm^{-1}, respectively, which could be assigned to the absorption of carboxyl groups of PMAA (Yang et al., 2005), protonated amino groups of CS (Hu et al., 2004), and Si–O of MSN (Morey et al., 2000). The bands at 1538 and 1406 cm^{-1} could be assigned to asymmetric and symmetric stretching vibrations of COO– anion groups, which verified that PMAA were dissociated into COO– groups and complexed with CS through electrostatic interaction to form polyelectrolyte complexes during the polymerization.

The thermogravimetric analysis (TGA) of MSN and MSN/CS-PMAA composite microspheres was also performed (Fig. 4). The TGA curves demonstrated that the weight loss of MSN was 11%, while that of MSN/CS-PMAA was 44.4%. Pure CS could be decomposed entirely at 800 °C (weight loss 98.8%). Thus, the content of CS-PMAA component was about 37.5 wt% in MSN/CS-PMAA composite microspheres. This result was in consistent with the scales of the core–shell structure observed by TEM.

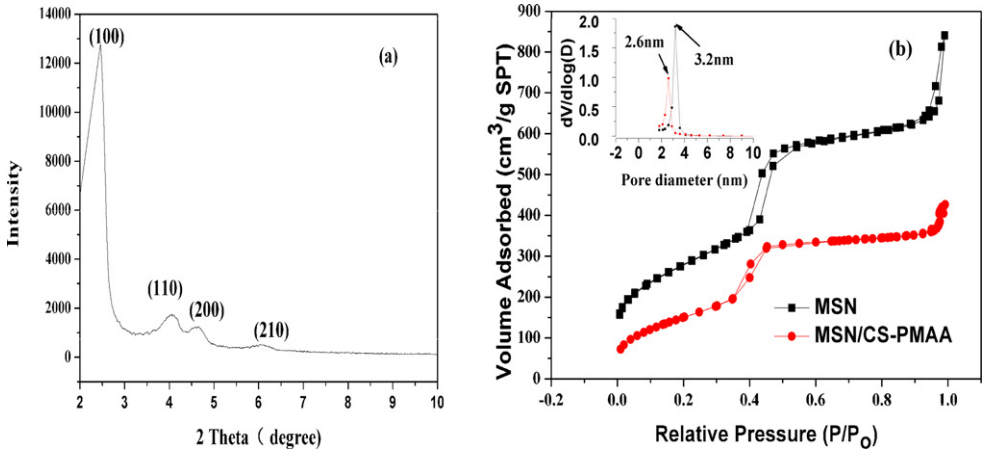

Fig. 2. XRD pattern of MSN (a) and nitrogen adsorption desorption isotherms result (b) of MSN and MSN/CS-PMAA.

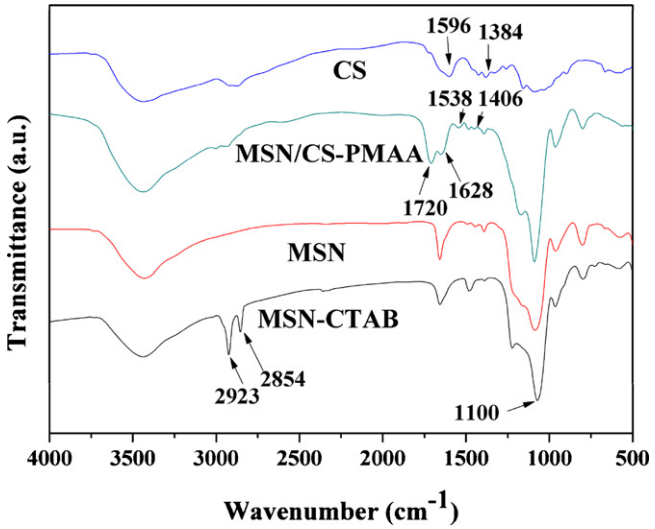

Fig. 3. FTIR spectra of MSN-CTAB (as-prepared MSN), MSN, MSN/CS-PMAA, and CS.

3.2. Influence of external parameters on the formation of composite microspheres

As demonstrated previously, physicochemical properties such as size, shell thickness and surface charges of vehicles can determine the cell viability and blood compatibility when applied in biological field (Dash et al., 2010). Herein, we undertook rigorous investigation to control the shell thickness, surface charges and sizes of the composite microspheres.

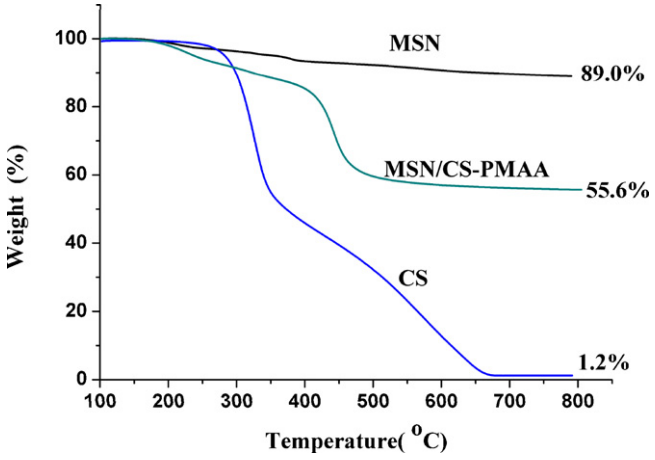

Fig. 4. TGA curves of MSN, CS and MSN/CS-PMAA.

Table 2
Particle size and zeta potential of the MSN/CS-PMAA composite microspheres prepared at different [–NH_2]/MAA.[a]

No.	[–NH_2]/MAA	Zeta potential (mV)	Hydrodynamic diameter (nm)[b]	PI[c]
a	1: 8	−48	728	0.69
b	1:4	−46	350	0.16
c	1:2	−42	425	0.21
d	1:1	−34	476	0.28
e	2:1	−21	503	0.31

[a] All the data was measured at pH 7.4 and 0.15 M sodium phosphate buffer solution.
[b] The diameter was determined at 25 °C by DLS.
[c] PI, polydispersity index, PI = $\langle\mu_2\rangle/\Gamma^2$.

Fig. 5 showed the TEM images of different MSN/CS-PMAA composite microspheres synthesized by varying the concentrations of MSN in the reaction system. With the increase of the concentration of MSN, the thickness of polymer nanoshell decreased (from left to right) from the approximately 10 nm (Fig. 5(a)) to nearly invisible. The TGA results (data not shown here) also confirmed the different thickness of the polymer nanoshell with the weight-loss of 57.5%, 44.4% and 26.9% at 800 °C when MSN concentrations were 1, 5 and 10 g/L, respectively. It was obvious that the more the amount of MSN in the reaction system, the less CS-PMAA assemblies allocated for each MSN. In addition, with more MSN amount, the ionic crosslinking and electrostatic shielding effect made the polyelectrolyte nanoshell gradually compact (Cha et al., 2003), which was verified by the DLS data with the hydrodynamic diameter of 425 nm, 358 nm and 320 nm for the composite microspheres at pH 7.4 when MSN concentrations were 1, 5 and 10 g/L.

Table 2 showed that with the decrease of the feeding ratio of [–NH_2]/MAA from 2:1 to 1:4, the zeta potential of the composite microspheres decreased from −21 to −46 mV, together with a decline of the hydrodynamic diameter from 503 to 350 nm and polydispersity index. Further decreasing the molar ratio of [–NH_2]/MAA to 1:8, the zeta potential of the composite microspheres decreased to −48 mV while the hydrodynamic diameter increased to 728 nm along with larger polydispersity index (PI = 0.69) was observed. These results revealed that the molar ratio of [–NH_2]/MAA may have an optimum point, but it was likely

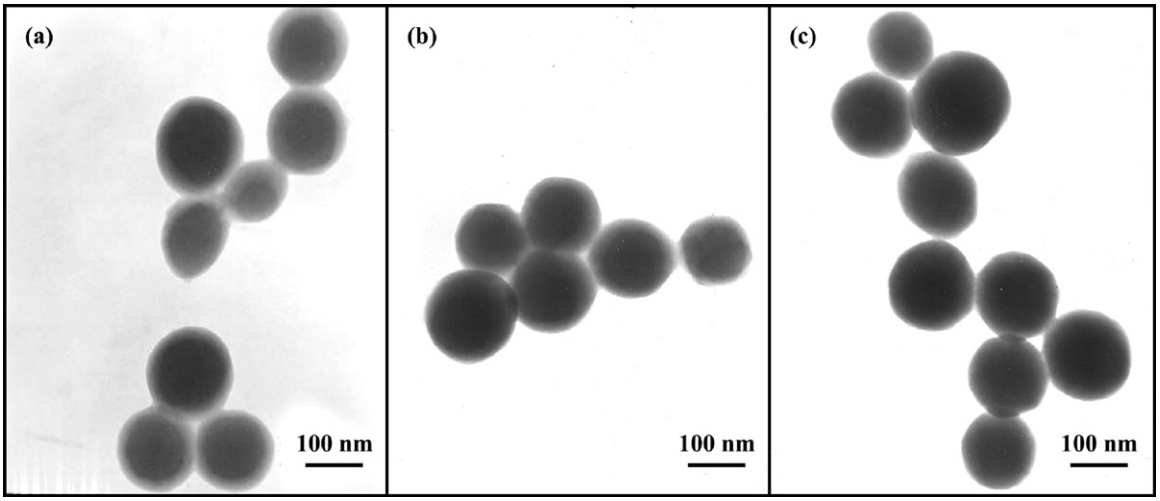

Fig. 5. TEM micrographs of MSN/CS-PMAA composite microspheres with different MSN concentration: (a) 1 g/L, (b) 5 g/L, (b) 10 g/L. The concentrations of CS and MAA were constant.

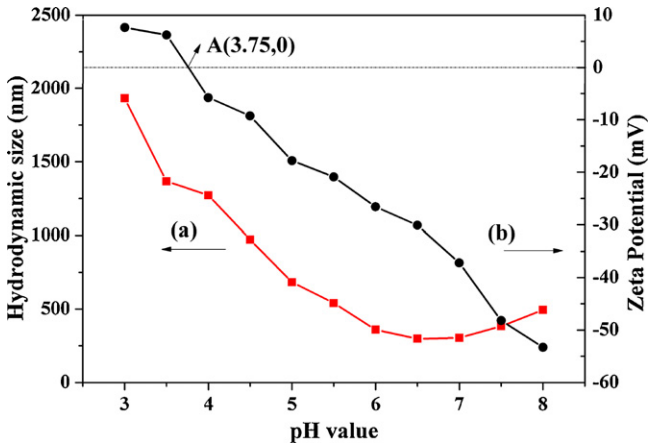

Fig. 6. The size (a) and zeta potential (b) of cross-linked MSN/CS-PMAA composite microspheres at different pH.

far away from the theoretical molar ratio that was close to 1 as one amino group coordinated with one carboxyl group. It was reported that at low pH value, PMAA existed in a highly compact and ultra-coil conformation (Soutar and Swanson, 1994). Taking it into consideration, we assumed that only part of the dissociative carboxyl groups in the chain segments interacted well with the protonated amino groups. When the molar ratio of [$-NH_2$]/MAA was 1:8, the excessive MAA would be polymerized to form dissociative PMAA and generated loose composite microspheres (De Moura et al., 2008), then the hydrodynamic diameter and size distribution became larger again (Table 2). Thus, the MSN/CS-PMAA composite microspheres prepared with [$-NH_2$]/MAA = 1:4 were chosen for further study.

3.3. Effect of pH and ionic strength on the stability of the composite microspheres

To investigate the pH-dependent behavior of the composite microspheres, the pH values of the dispersed medium was changed from 3 to 8. Fig. 6 exhibited the alteration tendency of zeta potentials and hydrodynamic diameters of MSN/CS-PMAA composite microspheres as a function of pH values. The trend of zeta potential showed a monotonous shape (Fig. 6(b)) while the hydrodynamic size showed a parabola shape (Fig. 6(a)) with pH variation. Similar results were demonstrated in the early report (Hu et al., 2005). Fig. 6(a) demonstrated that the hydrodynamic size reached a minimum at pH 6.5. Above pH 6.5, –COOH from PMAA would be dissociated and $-NH_2$ from chitosan would be deprotonated, increase of pH led to an increase of the ionization degree and charge density of the PMAA molecules, which would reduce the hydrogen bonding interactions and molecular linkages between the CS and PMAA chains, resulting in the increase of hydrodynamic size and the decrease of zeta potential simultaneously. Below pH 6.5, $-NH_2$ from chitosan would be protonated. With the decrease of pH value, the electrostatic repulsion of the formed protonated amino groups made the CS chains extended gradually, resulting in the swelling of the composite microspheres and the increase of the zeta potential (the decrease of the absolute value). The isoelectric points of MSN, CS and PMAA are 1.5 (Rosenholm and Linden, 2008), 6.5 (Ahn et al., 2001), and 4.9 (Pohlmeier and Haber-Pohlmeier, 2004), respectively. Point A in Fig. 6(b) at (3.75, 0) marked in the curve was used to determine the isoelectric point of MSN/CS-PMAA composite microspheres. Around the isoelectric point, zeta potential was near zero, the repulsion among microspheres was weaken, leading to the aggregation of the microspheres, so dramatic increase of the hydrodynamic diameter was observed.

Table 3
Particle size and size distribution of MSN/CS-PMAA composite microspheres in different salt concentration at pH 7.4.

NaCl concentration (mol/L)	Diameter (nm)[a]	PI[b]
0.01	297	0.05
0.05	307	0.06
0.10	330	0.10
0.15	356	0.12
0.30	427	0.19
0.60	575	0.42
1.00	748	1.00

[a] The diameter was determined at 25 °C by DLS.
[b] PI, polydispersity index, PI = $\langle\mu_2\rangle/\Gamma^2$.

The above results were very important since it not only proved the pH responsive property of MSN/CS-PMAA composite microspheres, but also indicated that the MSN/CS-PMAA composite microspheres were stable in the pH range of 5–8 and by controlling pH values, surface charges and hydrodynamic size can be easily controlled, which are very important for their application in drug delivery system.

Salt concentration also has a great influence on the stability of the composite microspheres, so it is important to examine the stability of the MSN/CS-PMAA composite microspheres at different NaCl concentrations. In Table 3, it can be found that the hydrodynamic diameters of the composite microspheres just had a slight increase when the salt concentrations increased from 0.01 to 0.30 M. Above 0.60 M, the hydrodynamic diameters of the composite microspheres increased rapidly together with the polydispersity indexes because more salt would screen the electrostatic charges on the surface of the composite microspheres (Stuart et al., 1998), leading to the destabilization of microspheres. The useful conclusion was that the MSN/CS-PMAA composite microspheres were stable in the physiological saline (0.15 M NaCl) and were promising for the further application as drug vehicles.

3.4. DOX loading and release

To evaluate the drug loading and releasing property of MSN/CS-PMAA composite microspheres, DOX, a classic anticancer drug, was used as a model drug. DOX was loaded into the composite microspheres at pH of 8. Previous studies have demonstrated that inorganic carriers such as MSN tended to have a high loading capacity but low encapsulation efficiency, opposite to the organic carriers such as micelles, liposomes and polymeric nanoparticles (Liu and Eisenberg, 2003; Matsumura and Maeda, 1986). However, in our case, the MSN/CS-PMAA composite microspheres held both high drug-loading capacity ($22.3 \pm 0.3\%$) and encapsulation efficiency ($95.7 \pm 2.0\%$). The drug was loaded by the composite microspheres may be attributed to the following reasons: (a) the drug loading experiment was performed at pH 8. At pH of 8, the composite microspheres were negative charged. The pK_a value of the anticancer drug DOX is 8.3 (Choucair et al., 2005), so the net charge of DOX was around zero, or a little positively charged at pH 8.0. There existed electrostatic attraction between DOX and the composite microspheres. In addition, the electrostatic repulsion among the adsorbed DOX molecules decreased evidently at pH 8, so nearly all the DOX molecules could be adsorbed into the composite microspheres (Chang et al., 2011). (b) The polymer shell (CS-PMAA) of the composite microspheres was in a loose state due to the hydrophilic effect of –COOH groups as well as the hydrophilic nature of chitosan, thus the drugs could diffuse into the composite microspheres (Yan et al., 2009). (c) There also existed hydrogen bonding complexation of the amino groups and hydroxyl groups in DOX molecules with the ionized $-COO^-$ groups in composite microspheres at pH 8.

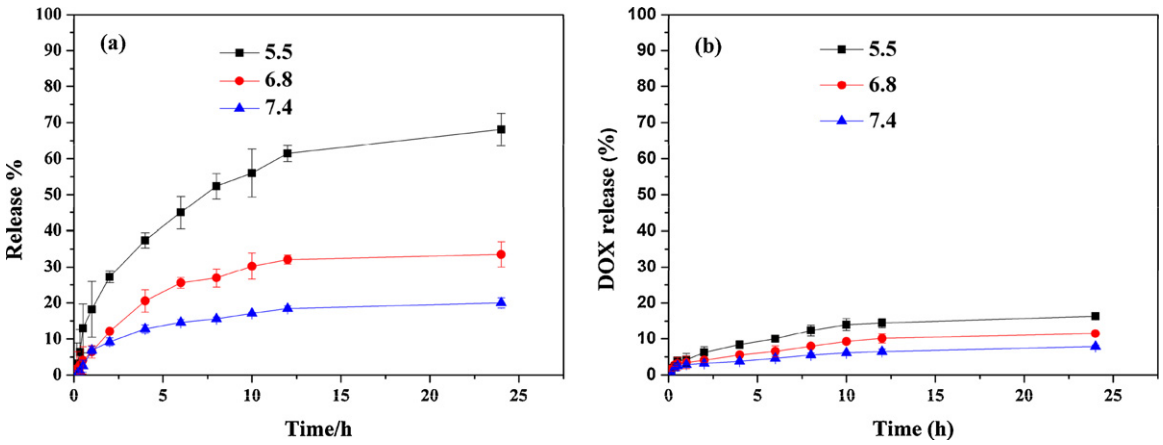

Fig. 7. Release profiles of DOX from MSN/CS-PMAA composite microspheres (a) and MSN (b) at pH values of 5.5, 6.8 and 7.4.

The release profiles of DOX@MSN/CS-PMAA were performed at pH values of 7.4 (blood circulation), 6.8 (tumor extracellular) and 5.5 (endosomes) for 24 h at 37 °C. Fig. 7(a) demonstrated that the DOX release rate was obviously pH dependent and increased with the decrease of pH. At pH 7.4, the release amount was quite low and only approximately 18 wt% was released in 24 h. At pH 6.8, the release profile curve leveled off after 12 h and the release amount was 34 wt% in 24 h. Intriguingly note that when pH decreased to 5.5, a faster release behavior was obtained and the release amount reached 70 wt% in 24 h, which was almost four times of that at pH 7.4. This is because the drug release from the composite microspheres was mainly determined by the effect of electrostatic interaction between DOX and polymer nanoshell. The pK_a of DOX is 8.3, so it was positively charged at the selected three pH values. On the whole, the higher the pH of the medium was, the more negative charges were on the surface of the composite microspheres (Fig. 6(b)), the stronger attraction existed between the positively charged DOX and the negatively charged carriers, so the more difficult for the loaded DOX to be released out of the composite microspheres.

As a comparison, the drug release experiments of DOX@MSN were also performed. Fig. 7(b) showed the drug release of DOX@MSN at pH values of 7.4, 6.8 and 5.5. Obviously, the differences in release amount among different pH were not as significant as that of DOX@MSN/CS-PMAA with the released drug amount of 8%, 11% and 16% in corresponding pH values after 24 h. Therefore, DOX@MSN/CS-PMAA displayed a more pronounced pH dependent property than DOX@MSN, and more drug molecules could be released for DOX@MSN/CS-PMAA system. Considering the fact that the tumor tissues are more acidic than the normal tissues, the prepared composite microspheres would be able to minimize the side effect of DOX. Combined with the specific drug release behavior and simultaneous high loading capacity and encapsulation efficiency for DOX, the MSN/CS-MAA composite microspheres are highly expected to be used in cancer treatment without frequent interval medication administrations.

3.5. *In vitro* cell assay and cell uptake

The results of DOX loading and releasing studies motivated us to further investigate the *in vitro* cellular cytotoxicity and uptake. The *in vitro* cytotoxicity of DOX@MSN/CS-PMAA to HeLa cells was investigated by MTT assay. When the pure composite microspheres were 0.1, 1, 10, 50, 100 μg/mL, the cell viability were 100 ± 5%, 100 ± 5%, 96 ± 5%, 96 ± 2%, 96 ± 14% for 24 h, respectively. As shown in Fig. 8, the blank carrier MSN/CS-PMAA showed no cytotoxicity on the HeLa cells even at 100 μg/mL after incubation for 24 h, suggesting that the MSN/CS-PMAA microspheres are biocompatible. Conversely, when the HeLa cells were treated with either the suspension of DOX-loaded MSN/CS-PMAA or a solution of pure DOX at high DOX concentration, significant decrease of the cancer cell viability was presented. Furthermore, it was interesting to note that the DOX loaded composite microspheres showed higher cytotoxicity than free DOX at the same drug dose. Also, the IC50 value (the concentration of drugs required to reduce cell growth by 50%) for HeLa cells was determined to be 1.1 μg/mL for free DOX and 0.5 μg/mL for DOX-loaded composite microspheres, respectively, so DOX@MSN/CS-PMAA showed a more efficient cytotoxicity than pure DOX to HeLa cells.

To observe the uptake of the MSN/CS-PMAA composite microspheres by HeLa cells, fluorescein isothiocyanate (FITC) was functionalized onto the mesoporous silica nanoparticles through a co-condensation method (Liong et al., 2008). FITC was first conjugated with aminopropyl triethoxysilane, and the product was then added into the system of preparation of MSNs to incorporate fluorescein into the composite microspheres. In Fig. 9, the green fluorescent signals arised from FITC dye and the red fluorescent signals derived from DOX. From Fig. 9(a3), green fluorescence showed MSN/CS-PMAA microspheres had been internalizated by

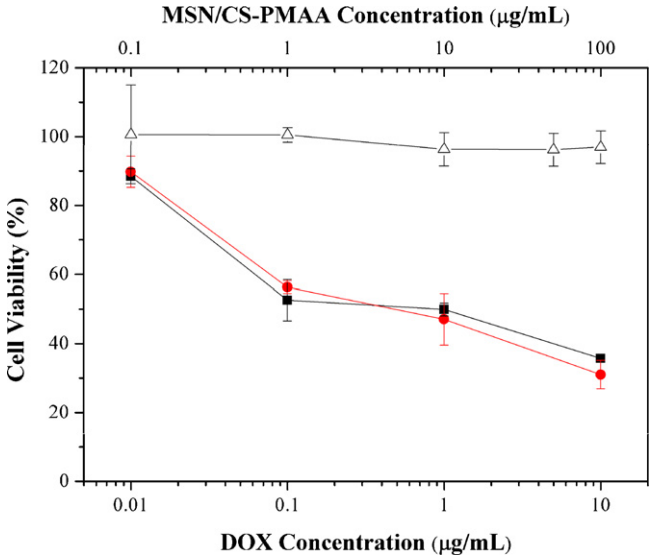

Fig. 8. Cell survival assay of HeLa cells: blank MSN/CS-PMAA (△), pure DOX (■) and DOX@MSN/CS-PMAA (●). The concentration of MSN/CS-PMAA was labeled at the top of the *x*-axis. (For interpretation of the references to color in this figure legend, the reader is referred to the web version of the article.)

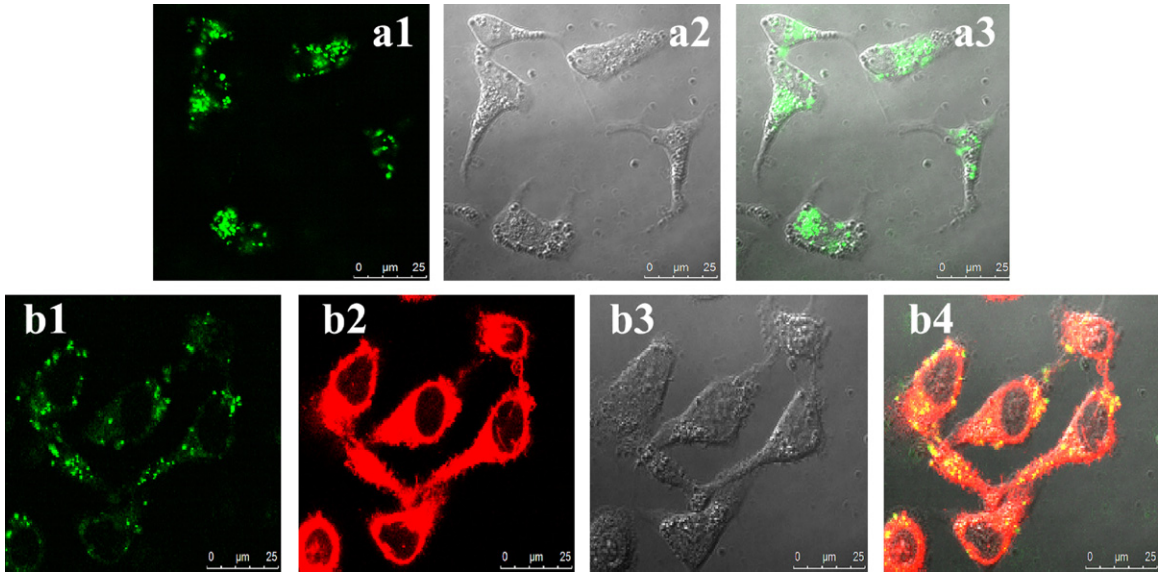

Fig. 9. The uptakes of MSN/CS-PMAA (a) and DOX@MSN/CS-PMAA (b) by HeLa cells were visualized by laser confocal scanning microscopy (incubation time: 3 h). MSN/CS-PMAA was labeled with FITC. Upper panel: (a1) FITC; (a2) differential interference contrast (DIC); and (a3) the merged image of (a1) and (a2). Lower panel: (b1) FITC; (b2) DOX; (b3) DIC; and (b4) the merged image of (b1), (b2) and (b3).

HeLa cell through endocytosis or macropinocytosis in 3 h (Vivero-Escoto et al., 2010). The internalization of DOX@MSN/CS-PMAA composite microspheres was demonstrated in Fig. 9(b). The yellow area (Fig. 9(b4)) showed the merged images of red area (DOX) and green area (FITC). The red area (DOX) was larger than the yellow area, indicating that DOX@MSN/CS-PMAA microspheres have been internalizated by HeLa cell, and DOX have been released from the drug-loaded microspheres effectively. Because endosomes are acidic microenvironment, and DOX have faster release rate at low pH in DOX@MSN/CS-PMAA system (see Section 3.4).

These results demonstrated that free MSN/CS-PMAA microspheres were biocompatible, while DOX@MSN/CS-PMAA had a good therapeutic efficacy. DOX@MSN/CS-PMAA can provide an added advantage of controlled release, wherein DOX molecules will be effectively released after the composite microspheres reaching the HeLa cells, minimizing systemic toxicity. This is very important as DOX is known of being highly toxic especially to the heart and the kidneys when administered in a free form (Azarmi et al., 2006).

4. Conclusions

In summary, a stable and highly effective drug delivery system mesoporous silica nanoparticles/chitosan-poly (methacrylic acid) (MSN/CS-PMAA) composite microspheres were prepared via *in situ* polymerization approach. The well defined core–shell composite microspheres were confirmed by the results from TEM observation, DLS, FTIR spectra, BET, and TGA measurements. The shell thickness, hydrodynamic diameters and surface charges of the obtained composite microspheres could be tuned by adjusting the feeding amount of MSN and the molar ratio of [$-NH_2$]/MAA in the reaction system. Doxorubicin hydrochloride (DOX) was applied as model drug to investigate drug loading and release behaviors. The composite microspheres possessed both high loading capacity (22.3%) and encapsulation efficiency (95.7%). The cumulative release of DOX@MSN/CS-PMAA showed a low leakage at pH 7.4 with only 18% amount was released after 24 h while significantly enhanced to 70% at pH 5.5. These results demonstrated that the drug release of the composite microspheres was pH-responsive apparently. The *in vitro* evaluation exhibited that the MSN/CS-PMAA microspheres were highly biocompatible and could be effectively taken up by HeLa cells. Overall, the simple and efficient nature of the approach, coupled with the capability to achieve good therapeutic efficacy, make the prepared polymer-coated microspheres a promising site specific anticancer drug delivery carrier.

Acknowledgements

We are grateful for the support of the National Science Foundation of China (grant Nos. 50403011, 20874015), the Shanghai Rising-Star Program (10QH1400200), and the Innovation Program of Shanghai Municipal Education Commission (09ZZ01).

References

Ahn, J.S., Choi, H.K., Cho, C.S., 2001. A novel mucoadhesive polymer prepared by template polymerization of acrylic acid in the presence of chitosan. Biomaterials 22, 923–928.

Angelos, S., Yang, Y.W., Patel, K., Stoddart, J.F., Zink, J.I., 2008. pH-responsive supramolecular nanovalves based on cucurbituril pseudorotaxanes. Angew. Chem. Int. Ed. 47, 2222–2226.

Ashley, C.E., Carnes, E.C., Phillips, G.E., Padilla, D., Durfee, P.N., Brown, P.A., Hanna, T.N., Liu, J.W., Phillips, B., Carter, M.B., Carroll, N.J., Jiang, X.M., Dunphy, D.R., Willman, C.L., Petsev, D.N., Evans, D.G., Parikh, A.N., Chackerian, B., Wharton, W., Peabody, D.S., Brinker, C.J., 2011. The targeted delivery of multicomponent cargos to cancer cells by nanoporous particle-supported lipid bilayers. Nat. Mater. 10, 389–397.

Azarmi, S., Tao, X., Chen, H., Wang, Z.L., Finlay, W.H., Lobenberg, R., Roa, W.H., 2006. Formulation and cytotoxicity of doxorubicin nanoparticles carried by dry powder aerosol particles. Int. J. Pharm. 319, 155–161.

Aznar, E., Marcos, M.D., Martinez-Manez, R., 2009. pH- and photo-switched release of guest molecules from mesoporous silica supports. J. Am. Chem. Soc. 131, 6833–6843.

Baldwin, A.D., Kiick, K.L., 2009. Polysaccharide-modified synthetic polymeric biomaterials. Biopolymers 94, 128–140.

Beck, J.S., Vartuli, J.C., Roth, W.J., Leonowicz, M.E., Kresge, C.T., Schmitt, K.D., Chu, C.T.W., Olson, D.H., Sheppard, E.W., McCullen, S.B., Higgins, J.B., Schlenker, J.L., 1992. A new family of mesoporous molecular-sieves prepared with liquid-crystal templates. J. Am. Chem. Soc. 114, 10834–10843.

Carniato, F., Bisio, C., Paul, G., Gatti, G., Bertinetti, L., Coluccia, S., Marchese, L., 2010. On the hydrothermal stability of MCM-41 mesoporous silica nanoparticles and the preparation of luminescent materials. J. Mater. Chem. 20, 5504–5509.

Casasus, R., Marcos, M.D., Martinez-Manez, R., 2004. Toward the development of ionically controlled nanoscopic molecular gates. J. Am. Chem. Soc. 126, 8612–8613.

Cha, J.N., Birkedal, H., Euliss, L.E., Bartl, M.H., Wong, M.S., Deming, T.J., Stucky, G.D., 2003. Spontaneous formation of nanoparticle vesicles from homopolymer polyelectrolytes. J. Am. Chem. Soc. 125, 8285–8289.

Chang, B.S., Shang, X.Y., Guo, J., Jiao, Y.F., Wang, C.C., Yang, W.L., 2011. Thermo and pH dual responsive, polymer shell coated, magnetic mesoporous silica nanoparticles for controlled drug release. J. Mater. Chem. 21, 9239–9247.

Chu, B., Wang, Z.L., Yu, J.Q., 1991. Dynamic light-scattering study of internal motions of polymer coils in dilute-solution. Macromolecules 26, 6832–6838.
Choucair, A., Soo, P.L., Eisenberg, A., 2005. Active loading and tunable release of doxorubicin from block copolymer vesicles. Langmuir 21, 9308–9313.
Colombo, P., Sonvico, F., Colombo, G., Bettini, R., 2009. Novel platforms for oral drug delivery. Pharm. Res. 26, 601–611.
Dash, B.C., Rethore, G., Monaghan, M., Fitzgerald, K., Gallagher, W., 2010. The influence of size and charge of chitosan/polyglutamic acid hollow spheres on cellular internalization, viability and blood compatibility. Biomaterials 31, 8188–8197.
De Moura, M.R., Aouada, F.A., Mattoso, L.H.C., 2008. Preparation of chitosan nanoparticles using methacrylic acid. J. Colloid Interface Sci. 321, 477–483.
De Vasconcelos, C.L., Bezerril, P.M., Dos Santos, D.E.S., Dantas, T.N.C., Pereira, M.R., Fonseca, J.L.C., 2006. Effect of molecular weight and ionic strength on the formation of polyelectrolyte complexes based on poly (methacrylic acid) and chitosan. Biomacromolecules 7, 1245–1252.
Engin, K., Leeper, D.B., Cater, J.R., Thistlethwaite, A.J., Tupchong, L., McFarlane, J.D., 1995. Extracellular pH distribution in human tumors. Int. J. Hyperthermia 11, 211–216.
Fleming, M.S., Mandal, T.K., Walt, D.R., 2001. Nanosphere-microsphere assembly: methods for core-shell materials preparation. Chem. Mater. 13, 2210–2216.
Gao, Q., Xu, Y., Wu, D., Sun, Y.H., Li, X.A., 2009. pH-responsive drug release from polymer-coated mesoporous silica spheres. J. Phys. Chem. C 113, 12753–12758.
Gao, Q.A., Xu, Y., Wu, D., Shen, W.L., Deng, F., 2010. Synthesis, characterization, and in vitro pH-controllable drug release from mesoporous silica spheres with switchable gates. Langmuir 26, 17133–17138.
Guo, J., Wang, C.C., Mao, W.Y., Yang, W.L., Liu, C.J., Chen, J.Y., 2008. Facile one-pot preparation and functionalization of luminescent chitosan-poly(methacrylic acid) microspheres based on polymer–monomer pairs. Nanotechnology 19, 315605–315610.
He, P., Davis, S.S., Illum, L., 1999. Chitosan microspheres prepared by spray drying. Int. J. Pharm. 187, 53–65.
Hong, C.Y., Li, X., Pan, C.Y., 2009. Fabrication of smart nanocontainers with a mesoporous core and a pH-responsive shell for controlled uptake and release. J. Mater. Chem. 19, 5155–5160.
Hu, Y., Jiang, X.Q., Ding, Y., Chen, Q., Yang, C.Z., 2004. Core-template-free strategy for preparing hollow nanospheres. Adv. Mater. 16, 933–937.
Hu, Y., Chen, Y., Chen, Q., Zhang, L.Y., Jiang, X.Q., Yang, C.Z., 2005. Synthesis and stimuli-responsive properties of chitosan/poly (acrylic acid) hollow nanospheres. Polymer 46, 12703–12710.
Lee, E.S., Oh, K.T., 2007. Tumor pH-responsive flower-like micelles of poly(L-lactic acid)-b-poly (ethylene glycol)-b-poly(L-histidine). J. Control. Release 123, 19–26.
Liong, M., Lu, J., Kovochich, M., Xia, T., Ruehm, S.G., Nel, A.E., Tamanoi, F., Zink, J.I., 2008. Multifunctional inorganic nanoparticles for imaging, targeting, and drug delivery. ACS Nano 2, 889–896.
Liu, F.T., Eisenberg, A., 2003. Preparation and pH triggered inversion of vesicles from poly(acrylic acid)-block-polystyrene-block-poly(4-vinyl pyridine). J. Am. Chem. Soc. 125, 15059–15064.
Liu, R., Liao, P.H., Liu, J.K., Feng, P.Y., 2011. Responsive polymer-based mesoporous silica as a pH-sensitive nanocarrier for controlled release. Langmuir 27, 3095–3099.
Liu, S., Maheshwari, R., Kiick, K.L., 2009. Polymer-based therapeutics. Macromolecules 42, 3–13.
Liu, T.Y., Hu, S.H., Liu, T.Y., Liu, D.M., Chen, S.Y., 2006. Magnetic-sensitive behavior of intelligent ferrogels for controlled release of drug. Langmuir 22, 5974–5978.
Lu, J., Liong, M., Li, Z.X., Zink, J.I., Tamanoi, F., 2010. Biocompatibility, biodistribution, and drug-delivery efficiency of mesoporous silica nanoparticles for cancer therapy in animals. Small 6, 1794–1805.
Matsumura, Y., Maeda, H., 1986. A new concept for macromolecular therapeutics in cancer-chemotherapy – mechanism of tumoritropic accumulation of proteins and the antitumor agent smancs. Cancer Res. 46, 6387–6392.
Medeiros, S.F., Santos, A.M., Fessi, H., Elaissari, A., 2011. Stimuli-responsive magnetic particles for biomedical applications. Int. J. Pharm. 403, 139–161.
Meng, H.A., Xue, M., Xia, T.A., Zhao, Y.L., Tamanoi, F., Stoddart, J.F., Zink, J.I., Nel, A.E., 2010. Autonomous in vitro anticancer drug release from mesoporous silica nanoparticles by pH-sensitive nanovalves. J. Am. Chem. Soc. 46, 12690–12697.
Morey, M.S., Bryan, J.D., Schwarz, S., Stucky, G.D., 2000. Pore surface functionalization of MCM-48 mesoporous silica with tungsten and molybdenum metal centers: perspectives on catalytic peroxide activation. Chem. Mater. 12, 3435–3444.
Pan, Y., Li, Y.J., Zhao, H.Y., Zheng, J.M., Xu, H., Wei, G., Hao, J.S., Cui, F.D., 2002. Bioadhesive polysaccharide in protein delivery system: chitosan nanoparticles improve the intestinal absorption of insulin in vivo. Int. J. Pharm. 249, 139–147.
Pichot, C., 2004. Surface-functionalized latexes for biotechnological applications. Curr. Opin. Colloid Interface Sci. 9, 213–221.
Pohlmeier, A., Haber-Pohlmeier, S., 2004. Ionization of short polymethacrylic acid: titration, DLS, and model calculations. J. Colloid Interface Sci. 273, 369–380.
Qiu, Y., Park, K., 2001. Responsive polymeric delivery systems. Adv. Drug Deliv. Rev. 53, 321–339.
Revilla, J., Elaissari, A., Pichot, C., Gallot, B., 1995. Surface functionalization of polystyrene latex particles with a liposaccharide monomer. Polym. Adv. Technol. 6, 455–464.
Rosenholm, J.M., Linden, M., 2008. Towards establishing structure-activity relationships for mesoporous silica in drug delivery applications. J. Control. Release 128, 157–164.
Schiffman, J.D., Schauer, C.L., 2007. Cross-linking chitosan nanofibers. Biomacromolecules 8, 594–601.
Schmaljohann, D., 2006. Thermo- and pH-responsive polymers in drug delivery. Adv. Drug Deliv. Rev. 58, 1655–1670.
Slowing, I.I., Trewyn, B.G., Lin, V.S.Y., 2007. Mesoporous silica nanoparticles for drug delivery and biosensing applications. J. Am. Chem. Soc. 129, 8845–8849.
Singh, K.P., Panwar, P., Kohli, P., Sanjesh, 2011. Liposome-mesoporous silica nanoparticles fused cores: a safer mode of drug carrier. J. Biomed. Nanotechnol. 7, 60–62.
Soutar, I., Swanson, L., 1994. Luminescence studies of polyelectrolyte behavior in solution. 3. Time-resolved fluorescence anisotropy measurements of the conformational behavior of poly(methacrylic acid) in dilute aqueous-solutions. Macromolecules 27, 4304–4311.
Stuart, M., Huck, W., Genzer, J., Müller, M., Ober, C., Stamm, M., 2010. Emerging applications of stimuli-responsive polymer materials. Nat. Mater. 9, 101–113.
Stuart, M.A.C., Besseling, N.A.M., Fokkink, R.G., 1998. Formation of micelles with complex coacervate cores. Langmuir 14, 6846–6849.
Vallet-Regi, M., Balas, F., Arcos, D., 2007. Mesoporous materials for drug delivery. Angew. Chem. Int. Ed. 46, 7548–7558.
Vallet-Regi, M., Ramila, A., del Real, R.P., Perez-Pariente, J., 2001. A new property of MCM-41: drug delivery system. Chem. Mater. 13, 308–311.
Vivero-Escoto, J.L., Slowing, I.I., Trewyn, B.G., Lin, V.S.Y., 2010. Mesoporous silica nanoparticles for intracellular controlled drug delivery. Small 6, 1952–1967.
Wang, Y., Bansal, V., Zelikin, A.N., Caruso, F., 2008. Templated synthesis of single-component polymer capsules and their application in drug delivery. Nano Lett. 8, 1741–1745.
Wang, Y.J., Yu, A.M., Caruso, F., 2005. Nanoporous polyelectrolyte spheres prepared by sequentially coating sacrificial mesoporous silica spheres. Angew. Chem. Int. Ed. 44, 2888–2892.
Wu, Y., Guo, J., Yang, W.L., Wang, C.C., Fu, S.K., 2006. Preparation and characterization of chitosan-poly(acrylic acid) polymer magnetic microspheres. Polymer 47, 5287–5294.
Yan, E.Y., Ding, Y., Chen, C.J., Li, R.T., Hu, Y., Jiang, X.Q., 2009. Polymer/silica hybrid hollow nanospheres with pH-sensitive drug release in physiological and intracellular environments. Chem. Commun. 19, 2718–2720.
Yang, Q., Wang, S.H., Fan, P.W., Wang, L.F., Di, Y., Lin, K.F., Xiao, F.S., 2005. Determination of outer membrane protein of *Aeromonas hydrophila* by pH controlled phase separation fluoroimmunoassay. Chem. Mater. 17, 5999–6003.
Zhao, Y.L., Li, Z.X., Kabehie, S., Botros, Y.Y., Stoddart, J.F., Zink, J.I., 2010. pH-operated nanopistons on the surfaces of mesoporous silica nanoparticles. J. Am. Chem. Soc. 132, 13016–13025.